J. Phys. Ther. Sci. 29: 590–597, 2017

The Journal of Physical Therapy Science

Original Article

Long-term histopathological developments in knee-joint components in a rat model of osteoarthritis induced by monosodium iodoacetate

Ikufumi Takahashi, RPT, PhD[1, 2)*], Taro Matsuzaki, RPT, PhD[3)], Masahiro Hoso, MD[3)]

[1)] *Section of Rehabilitation, Kanazawa University Hospital: 13-1 Takaramachi, Kanazawa, Ishikawa 920-8641, Japan*
[2)] *Department of Motor Function Analysis, Human Health Sciences, Graduate School of Medicine, Kyoto University, Japan*
[3)] *Faculty of Health Sciences, Institute of Medical, Pharmaceutical and Health Sciences, Kanazawa University, Japan*

Abstract. [Purpose] This study was performed to evaluate the long-term histopathological changes in knee-joint components including synovial membrane and joint capsule in a rat model of osteoarthritis (OA) induced by monosodium iodoacetate (MIA). [Subjects and Methods] Fifty male rats were used. OA was induced through intra-articular injection of MIA, and ten rats were randomly allocated to each of five groups induced with OA for 1, 2, 4, 6, or 8 weeks. At the end of each period, the knee components were examined histopathologically. [Results] After 1 and 2 weeks, chondrocytes were weakly stained. After 4 weeks, fibrillation, fissuring, and eburnation were observed, whereas after 6 weeks, chondrocyte clustering and osteophyte formation were detected. In the synovial membrane, the proliferation of spindle-shaped cells and a multilayered structure of the surface cells were observed at 1 and 2 weeks, but the degree of these changes decreased over time. In the joint capsule, a narrowing of the space between collagen fiber bundles was observed at 4–8 weeks. [Conclusion] The long-term histopathological changes of the joint components observed in a rat model of OA induced by MIA were similar to those detected in OA, but differed at specific times and tissues.

Key words: Osteoarthritis, Monosodium iodoacetate, Histopathology

(This article was submitted Nov. 22, 2016, and was accepted Dec. 15, 2016)

INTRODUCTION

Osteoarthritis (OA) is the most common form of degenerative joint disease and a leading cause of pain and chronic physical disability in elderly people[1)]. OA presents a multifactorial etiology, and can be considered the product of interactions between systemic, mechanical, and local factors within a joint[1)]. It is a chronic disease, which develops progressively over a span of decades and eventually leads to joint failure[2)].

Several previous experimental studies have focused on the histopathological changes of the articular cartilage and subchondral bone in OA. For example, Hayami et al. characterized subchondral bone remodeling, cartilage damage, and osteophytosis during disease progression in the anterior cruciate ligament transection (ACLT) model either alone or in combination with resection of medial menisci[3)]. Janusz et al. studied the effect of matrix metalloproteinase inhibitors in mono-iodoacetate (MIA)-induced arthritis in rats, and reported that MMP inhibitors are partially protective against cartilage

*Corresponding author. Ikufumi Takahashi (E-mail: t_ikuhumi@med.kanazawa-u.ac.jp)

and subchondral bone damage induced by iodoacetate[4]. Thus, previous studies have typically evaluated the histopathological changes of articular cartilage and subchondral bone as one interpretation of the results of treatments. However, in most of these studies, the experimental period was short (2–4 weeks), and in recent years, only a few basic studies have focused on the histological natural history in OA over a period of >8 weeks[5–9].

How joint components other than the articular cartilage and subchondral bone, such as the synovial membrane and the joint capsule, change histopathologically with OA development is another question that remains unanswered. Synovitis contributes to OA progression. Scanzello et al. reported that the low-grade synovitis of OA is associated with increased symptoms such as pain and degree of joint dysfunction, and might promote rapid cartilage degeneration[10]; they further identified four patterns of OA-associated "synoviopathy": hyperplastic, fibrotic, detritus-rich, and inflammatory[10]. However, the time-dependent histopathological changes of the synovial membrane remain unreported. Similarly, the histopathological changes of the joint capsule have not been elucidated thus far; however, the limitation of the joint range of motion in OA patients is widely recognized, and in the contracture model developed using joint immobilization, the joint capsule has been reported to change histopathologically. Matsuzaki et al. reported that the joint capsule in the immobilization group showed a narrowing of the collagen bundles in interstitial spaces[11], and Watanabe et al. observed that the thickness of the joint capsule had increased by 4 weeks of immobilization and progressed with prolongation of the immobilization period[12]. Based on these factors, the joint capsule might be considered to change histopathologically in OA, but previous studies have not described either the histopathological changes of these joint components in OA, or the mechanism and process of the degeneration of joint components that are accompanied by OA development.

Animal-model systems represent a crucial adjunct and surrogate for studies of OA in humans. These systems not only provide a means of studying OA pathophysiology, but also aid in the development of therapeutic agents and biological markers for OA diagnosis and prognosis. The OA animal models belong to three general categories of in vivo OA models: naturally occurring OA models (including genetically modified animals); models for the initiation or acceleration of joint degeneration developed using surgery or other trauma; and models developed through intra-articular injection of chondrotoxic or proinflammatory substances[2]. Among these, the chemical model presents certain advantages such as high reproducibility and accuracy, mildly invasive procedures, easy implementation, and most rapidly progressing OA[5]. In rats, the MIA model is well established, and the induced OA resembles human degenerative OA in terms of the histological and pain-related behavior[5]. MIA is a metabolic inhibitor that breaks down the cellular aerobic glycolysis pathway and, consequently, induces cell death by inhibiting the activity of glyceraldehyde-3-phosphate dehydrogenase in chondrocytes[5–9]. Intra-articular injection of MIA leads to a reduction in the number of chondrocytes and subsequent histological and morphological articular alterations that are similar to the changes in human OA[5–9]. However, previous research has rarely focused on the histopathological changes of articular joint components, including the synovial membrane and the joint capsule, in the MIA-induced OA model. Therefore, in this study, we investigated the long-term histopathological developments in knee-joint components by using a rat model of OA induced by MIA.

SUBJECTS AND METHODS

Fifty male Wistar rats (9 week old, 272.8 ± 8.5 g) were evaluated in this study. The animals were housed under normal conditions for 1 week before the start of the experiments in order to acclimatize them to the environment. One or two rats were housed per cage, in a sanitary ventilated room with controlled temperature, humidity, and a 12/12-h light-dark cycle, and food and water were provided ad libitum. This investigation was approved by the Animal Research Committee of the Kanazawa University Graduate School of Medicine, Kanazawa, Japan (Approval No.153501). All animal care and treatment procedures were performed in accordance with the Guidelines for the Care and Use of Laboratory Animals at Kanazawa University.

OA was induced through a single intra-articular injection of MIA as described previously[4, 7–10]. In rats, 1 mg of MIA has been demonstrated to be the maximal effective dose for inducing OA[6]. In our pilot study, rats were anesthetized by intraperitoneally injecting them with 40 mg/kg sodium pentobarbital. The left knees were shaved and disinfected, and then an incision was made at the center of the knee to expose the patellar ligament. Each rat was positioned on its back and the left leg was flexed 90° at the knee. The patellar ligament was palpated below the patella and MIA was injected into this region; 1 mg of MIA (Sigma, St. Louis, MO, USA; cat no. I2512) was dissolved in sterile saline and administered in a volume of 50 µl by using a 29-gauge 0.5-inch needle. Care was taken to ensure that the needle was not advanced too far into the cruciate ligaments. However, when pulling out the injector, the solution spilled over the capsule. Moreover, when the left knee was dissected at 1 day post-surgery, the subcutaneous tissue in most rats was found to be wet (the right knee had no wetness). Therefore, we concluded that the saline volume was excessive, and, consequently, in the main study, we injected the 50 rats with 1.0 mg of MIA dissolved in 30 µl of saline. When their left knees were subsequently dissected at 1, 2, 4, 6, and 8 weeks after the MIA administration, the subcutaneous tissue of the knee was not wet in any of the rats.

The five experimental groups contained 10 rats each, which were sacrificed—through intraperitoneal injection of a lethal dose of sodium pentobarbital—at 1, 2, 4, 6, or 8 weeks after the MIA administration. Immediately after the animals died, left hind limbs were disarticulated at the hip joint, and all knees were fixed in 10% neutral-buffered formalin for 72 h and decalcified using Decalcifying Solution A (7% w/v $AlCl_3 6H_2O$, 5% formic acid, and 8.5% HCl. Plank-Rychlo Method, Wako

Pure Chemical Industries, Ltd., Osaka, Japan) for 72 h. The knees were excised, deacidified in 5% sodium sulfate solution for 72 h, dehydrated in 100% ethanol after washing with water, embedded in paraffin wax, and then sectioned coronally (3 μm). These slides were stained separately with hematoxylin and eosin (H&E) and 0.05% toluidine blue for 10 min, and then sequentially dehydrated in 70%, 80%, 90%, and 100% ethanol. Finally, sections were cleared in xylene. For histology, one representative slice was chosen. A light microscope and a digital camera (BX-51 and DP-50; Olympus Corporation, Tokyo, Japan) were used to image and examine the articular cartilage in the medial femorotibial joint, and the synovial membrane and joint capsule in medial knee compartments. The histopathological features were evaluated by a single blinded pathologist. The normal and histopathological features in OA were examined for cell and matrix appearance according to previous studies. Figure 1 shows the normal articular cartilage, subchondral bone, synovial membrane, and joint capsule samples that were stained with H&E and toluidine blue for histopathological analysis. Normal articular cartilage and subchondral bone are composed of a small number of cells (chondrocytes) embedded in an abundant extracellular matrix[13]. The extracellular matrix consists predominantly of type-II collagen, proteoglycans, and water, together with comparatively smaller amounts of other collagen types and non-collagenous proteins[14]. Histologically, the articular cartilage is divided into 4 zones: the tangential layer, the transitional layer, the radial layer, and the calcified layer[14]; these zones are distinguished by the shape of the chondrocytes and the arrangement of type-II collagen fibers[14]. A microscopically distinct line—the tidemark—separates the lower radial zone from the underlying zone of calcified cartilage, and deep inside the calcified cartilage lies the subchondral bone plate[13]. In the normal synovial membrane, the synovium is composed of two layers: an intimal component of 1–3 discontinuous cell layers of synoviocytes (or synovial-lining cells, which are fibroblasts and macrophages) featuring an incomplete basement membrane; and an outer subintimal layer that merges with the fibrous joint capsule and contains nerves, lymphatics, and vasculature[15]. The normal joint capsule is composed of interlacing bundles of parallel fibers of collagen, and the capsule is perforated by vessels and nerves[13]. Similarly, the histopathological features in OA were examined for cell and matrix appearance according to previous studies[11, 12, 16–18]. For example, the specific features detected in the articular cartilage are fibrillation, fissuring, and eburnation; in the synovial membrane, proliferation of spindle-shaped cells and a multilayered structure of the surface cells; and in joint capsules, infiltration of inflammatory cells and a narrowing of the space between collagen fiber bundles.

RESULTS

All animals were conscious and started to move within several hours after the surgery. No rat showed signs of knee infection or swelling or died during the experimental period. Thus, the inflammation was macroscopically and microscopically well controlled. The histopathological features are summarized in Table 1.

In cartilage degeneration (Figs. 2, 3, and 4(A), (B), (C), (E)), in sections stained with H&E, we detected weak staining of chondrocyte nuclei in the tangential and transitional layers, and noted nuclear enlargement, disintegration of nuclei, and differences in nuclear size at 1 week. The extent of these detected changes differed at the site of the articular cartilage. However, the chondrocytes in the lacuna in the radial layer had survived without degeneration. In toluidine blue staining, we observed weak staining of the cartilage matrix from the radial layer to the tangential layer, but a normal degree of staining was retained in the calcified layer. At 2 weeks, H&E staining yielded results similar to those obtained after 1 week: chondrocyte nuclei were again weakly stained in the tangential and transitional layers, and the chondrocytes in the lacuna in the radial layer had survived without degeneration, but chondrocyte clusters were not observed. By contrast, toluidine blue staining of the cartilage matrix was weaker after 2 weeks than after 1 week. At 4 weeks, H&E staining revealed fibrillation, fissuring, and eburnation in the loading portion. Moreover, weak staining of chondrocyte nuclei was observed in the tangential and transitional layers, and chondrocyte clusters were not detected. In toluidine blue staining, no staining of the cartilage matrix was observed from the radial layer to the tangential layer, but a normal degree of staining was retained in the calcified layer. At 6 weeks, H&E staining revealed, as at 4 weeks, fibrillation, fissuring, and eburnation in the loading portion. In toluidine blue staining, in certain specimens, chondrocyte clusters in osteophytes were observed in the margin of the articular cartilage. However, no stained cartilage matrix was observed from the radial layer to the tangential layer in the loading portion. At 8 weeks, eburnation in the entire loading portion and joint deformity were observed. The cartilage matrix had disappeared: no staining of the cartilage matrix was detected in any of the layers in toluidine blue staining. In all specimens, chondrocyte clusters and osteophytes were observed in the margin of the articular cartilage.

In subchondral bone degeneration (Figs. 2, 3, and 4(D)), the area of the calcified layer had increased, and thus the integration of the structure and the layers was disturbed at 1 week. Moreover, vascularization into the calcified layer was observed. At 2 weeks, a portion of the tidemark had disappeared, and the expansion and vascularization of the calcified layer were also observed. After 4 weeks, together with the fissuring and eburnation of the articular cartilage, the cartilage matrix and the tidemark had disappeared, and expansion and vascularization of the calcified layer were observed continuously over the experimental time course.

In synovial membrane inflammation (Fig. 5), we observed the proliferation of spindle-shaped cells in the surface layer of the synovial membrane and a multilayered structure of the surface cells at 1 week. Furthermore, possible mild infiltration of inflammatory cells was detected, and congestion and vasodilatation of vessels were also observed. At 2–4 weeks, as at 1

Table 1. Summary of histopathological developments in knee components

			1 wk	2 wk	4 wk	6 wk	8 wk
Articular cartilage	Weak staining of chondrocytes		10	10	10	8	9
	Weak staining of cartilage matrix by toluidine blue	in tangential zone	8	10	10	7	4
		in deep zone	2	0	4	7	4
	Chondrocyte clustering	in loading portion	0	0	0	0	0
		in margin	0	1	0	5	10
	Fibrillation		0	1	9	3	4
	Fissuring		0	0	9	3	3
	Eburnation		0	0	7	5	7
	Deformity		0	1	1	2	3
Subchondral bone	Disappearance of tidemark		1	10	9	9	9
	Calcification in subchondral bone		10	10	9	10	10
	Vascularization		5	10	6	4	10
Synovial membrane	Proliferation of spindle-shaped cells		10	10	10	8	6
	Multilayered structure of surface cells		10	10	9	4	4
	Deposition of fibrin		1	0	1	0	0
	Infiltration of inflammatory cells		10	9	8	6	4
	Congestion and vasodilatation of vessels		6	10	8	3	3
Joint capsule	Infiltration of inflammatory cells		10	4	2	1	1
	Congestion and vasodilatation of vessels		8	9	8	9	5
	Narrowing of space between collagen fiber bundles		0	0	1	7	9

Numerals represent the number of animals.

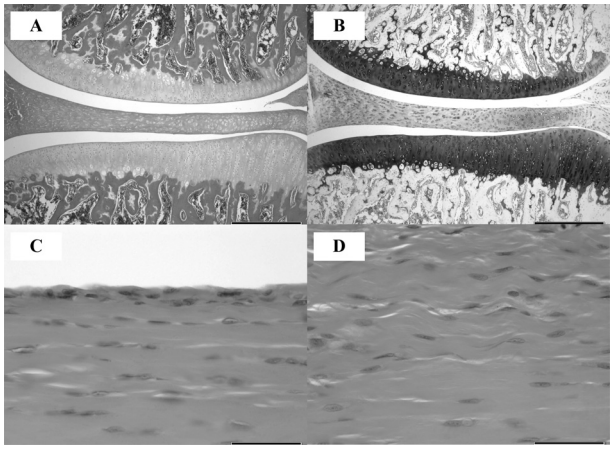

Fig. 1. Histopathological analysis of normal joint components
Articular cartilage stained with hematoxylin and eosin (H&E) (A) and toluidine blue (B). H&E staining of synovial membrane (C) and joint capsule (D). Scale bar=500 μm (A, B) and 50 μm (C, D)

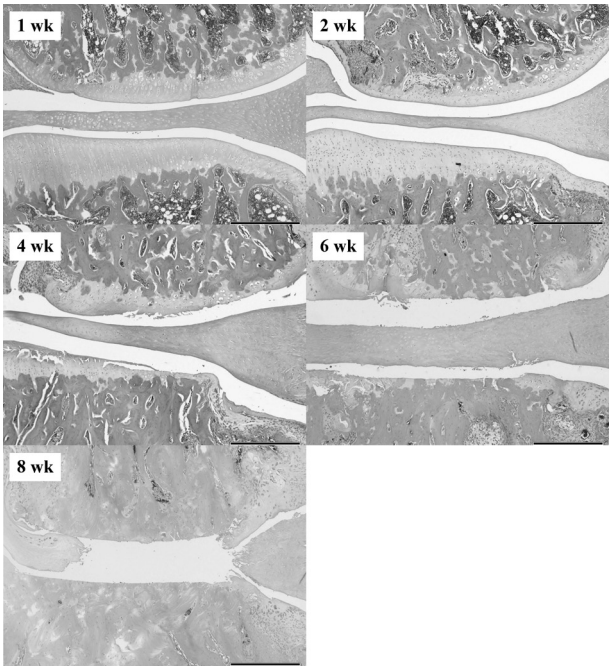

Fig. 2. Histopathological (H&E) staining of coronal sections of the medial femorotibial joint
Scale bar=500 μm

week, we observed the proliferation of spindle-shaped cells, the multilayered structure of the surface cells, the possible mild infiltration of inflammatory cells, and the congestion and vasodilatation of vessels; however, examination after 6 and 8 weeks revealed that the degree of all of these observed changes had decreased over the experimental time course.

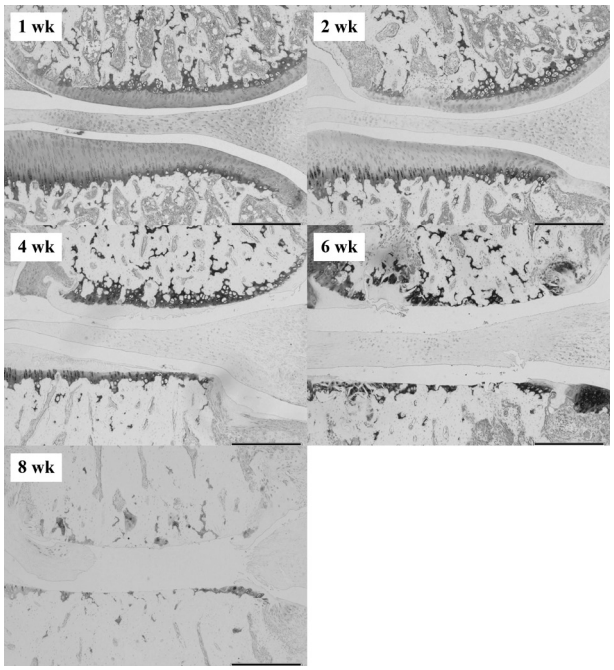

Fig. 3. Histopathological (toluidine blue) staining of coronal sections of the medial femorotibial joint
Scale bar=500 μm

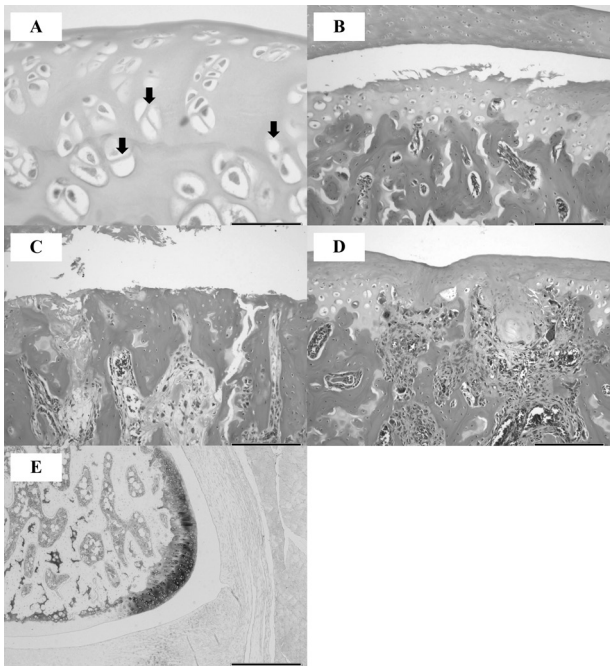

Fig. 4. Representative histopathological features of the articular cartilage
The panels show weak staining of chondrocytes (A; black arrows), fibrillation and fissuring (B), eburnation (C), vascularization into the articular cartilage (D; white arrows), and osteophyte formation (E). Scale bar=50 μm (A), 200 μm (B, C, D), and 500 μm (E)

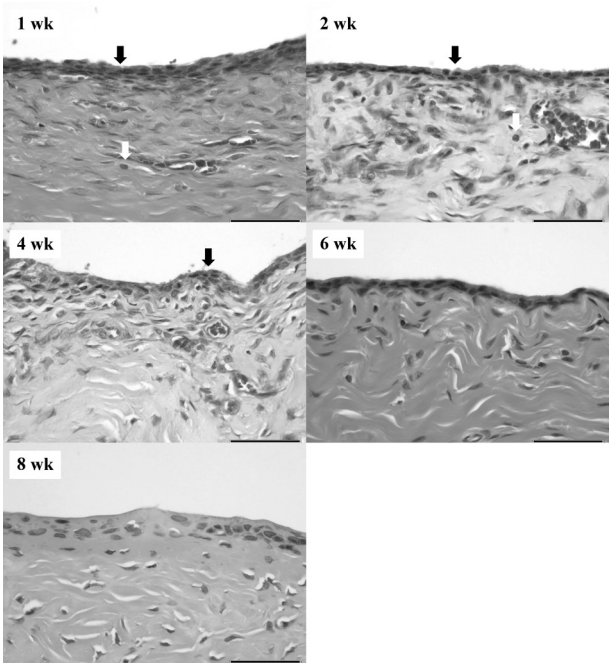

Fig. 5. Histopathological (H&E) staining of the synovial membrane
From 1 to 4 weeks, proliferation of spindle-shaped cells in the surface layer and a multilayered structure of the surface cells were observed (black arrows). Moreover, possible mild infiltration of inflammatory cells was detected (white arrows). Scale bar=50 μm

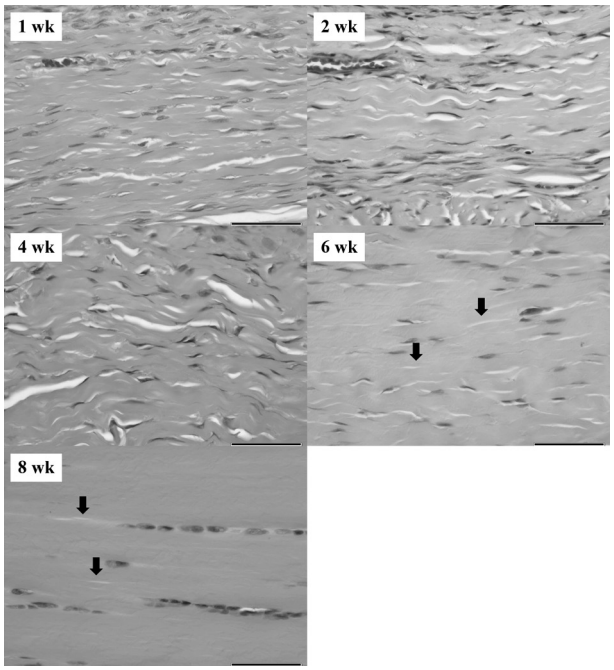

Fig. 6. Histopathological (H&E) staining of the joint capsule
A narrowing of the space between collagen fiber bundles was observed at 4 weeks. At 6 and 8 weeks, the degree of this narrowing of the space in the joint capsule had increased (black arrows). Scale bar=50 μm

In joint capsule (Fig. 6), congestion and vasodilatation of vessels were detected after 1 week and lasted continuously up to 8 weeks. Conversely, although possible mild infiltration of inflammatory cells was observed after 1 week, this decreased over time and had almost disappeared after 4 weeks. At 4 weeks, a narrowing of the space between collagen fiber bundles was observed, and at 6 and 8 weeks, the degree of the narrowing had increased further.

DISCUSSION

The rat model of OA induced by MIA is a well-established, widely used model. Guzman et al. created this MIA-induced OA rat model and described the histopathology in the subchondral bone and cartilage[8], and reported that the early time points were characterized by areas of chondrocyte degeneration and necrosis that occasionally involved the entire thickness of the articular cartilage[8]. They concluded that intra-articular injection of MIA induces a loss of the articular cartilage with the progression of subchondral bone lesions, and further that this model offers a rapid and minimally invasive method to reproduce OA-like lesions in a rodent species[8]. In our study, the histopathological change of weak chondrocyte staining that we observed after 1 and 2 weeks was similar to the results of the previous study, and the results obtained here after 6 weeks showed typical OA changes, such as fibrillation, fissuring, eburnation, calcification of the subchondral bone, and osteophyte formation, which again supported the previous study results.

At all experimental time points in this study, weak staining of chondrocyte nuclei was observed in the tangential and transitional layers, and nuclear enlargement, disintegration of nuclei, and differences in nuclear size were detected unaccompanied by inflammatory cell infiltration. This finding could potentially suggest chondrocyte necrosis or apoptosis. In previous studies, chondrocyte death in OA was reported to occur due to apoptosis and necrosis[19, 20]. Moreover, Jiang et al. reported that MIA-induced apoptosis in primary rat chondrocytes occurred primarily through reactive oxygen species production and mitochondria-mediated caspase-3 activation[6]. However, in this study, the observed histopathological changes of chondrocytes did not indicate either necrosis or apoptosis. Moreover, we observed a disappearance of the tidemark accompanied by vascularization into the articular cartilage in the early phase and a delay of osteophyte formation, and these findings also differed from those of the previous studies. Guzman et al. reported that calcification of the subchondral bone was observed at 56 days[8]. Chondrocytes produce inhibitors of angiogenesis, such as tissue inhibitor of metalloproteinase[21, 22]. Angiogenesis, mediated by the action of vascular endothelial growth factor, is known to be a contributing factor in the pathogenesis of OA[23]. The angiogenesis inhibitors prevent vessels from penetrating the articular cartilage, but in OA, angiogenesis from the subchondral bone was reported to breach the tidemark and enter into the articular cartilage[22]. Thus, a reduction in the production of angiogenesis inhibitor due to metabolism deterioration in chondrocytes might result in the penetration of the articular cartilage by vessels from the subchondral bone, and the tidemark might disappear in conjunction with the calcification of the subchondral bone.

In this study, we found that osteophyte formation occurred at a later time than reported in previous studies. In surgical OA models such as the ACLT model, the osteophyte forms more quickly than in chemical models such as the MIA model. A few previous studies conducted using surgical OA models reported that the osteophyte forms within a few days to a few weeks after surgical interventions such as ACLT[24–27]. By contrast, Ferland et al. reported that osteophyte formation was observed at 28 days in a rat model of OA induced by MIA[26], and in this study, we detected osteophyte formation at 6–8 weeks after MIA administration. Several studies have described the mechanism of osteophyte formation. The osteoblasts, chondrocytes, fibroblasts, synovial cells, and mesenchymal stem cells that are present in the periosteum are all involved in osteophyte formation[28, 29], a process that is regulated by numerous growth factors and cytokines, such as transforming growth factor-β and bone morphogenetic protein secreted by chondrocytes and synovial cells[28, 29]. Therefore, MIA administration might affect these regulatory mechanisms and thereby lead to the delay of osteophyte formation.

The time-dependent histopathological changes of the synovial membrane and joint capsule described here are new observations. In the synovial membrane, the histopathological features typically observed in OA are synovial lining hyperplasia, villous hyperplasia, fibrosis, and perivascular mononuclear cell infiltration[10, 30, 31]. However, in the case of the joint capsule, the features that develop in OA have not been previously elucidated. In this study, we observed inflammatory cell infiltration, hyperplasia of spindle-shaped cells, a multilayered structure of surface cells, angiogenesis, congestion and vasodilatation of vessels, and a narrowing of the space between collagen fiber bundles, and all of these histopathological changes—except for the narrowing of the space between collagen fiber bundles—became progressively milder over time. We suggest that these histopathological changes represent a response to the tissue impairment induced by MIA toxicity. According to the Globally Harmonized System of Classification and Labeling of Chemicals[32], MIA produces acute toxicity, and this toxicity is considered to induce a tissue response.

In this study, we obtained three intriguing and noteworthy results: one, in the early phase (i.e., at 1 week after surgery), the degree of toluidine blue staining of the cartilage matrix was decreased. Two, although most of the chondrocytes underwent degeneration over time, chondrocytes were regenerated as their clusters formed in the osteophyte at 6–8 weeks after surgery (Fig. 4 (E)). Chondrocytes were previously reported to exhibit poor regeneration potential[13, 14], but the findings of this study suggest that chondrocyte metabolism is not slow and that chondrocytes can present a certain level of regeneration potential in specific situations. Three, the appearance of cartilage regeneration in the loading portion was distinct from that in the margin of the cartilage: cartilage in the loading portion appeared necrotic, and chondrocyte regeneration and clustering were not

observed; by contrast, in the cartilage margin, chondrocyte clustering, regeneration of chondrocytes and the cartilage matrix, and osteophyte formation were observed. This finding suggests that mechanical stress—such as loading—might influence cartilage destruction and that the periosteum and the synovial membrane near the margin of the articular cartilage affect cartilage regeneration.

One limitation of this study is that, while we performed a detailed histopathological analysis of the joint component changes, we did not evaluate them quantitatively using a histological scale for cartilage degeneration and a morphological measurement for the space between collagen fibers in the joint capsule. Further study is needed to provide a detailed quantitative evaluation.

In conclusion, overall, the histopathological changes of the joint components observed here in a rat model of OA induced by MIA were similar to those detected in OA, but differed at specific times and tissues. The MIA-induced OA rat model was previously reported to represent an artificial model developed using a chemical agent, and the model was reported to be distinct in certain aspects from the naturally occurring OA model[2, 5, 16]. However, when selected appropriately, a rat model of OA induced by MIA can serve as a highly favorable model because it offers high reproducibility and accuracy, and involves only mildly invasive procedures. Further investigation is required to clarify the histopathological changes in OA to determine the potential of cartilage regeneration and the influence of mechanical stress on cartilage repair.

Author contributions

All authors have made substantial contributions to (1) the conception and design of the study, acquisition of data, or analysis and interpretation of data; (2) drafting the article or critically revising it for important intellectual content; and (3) final approval of the submitted version of the manuscript.

The specific contributions of the authors are as follows:

(1) Conception and design of the study: IT, TM, and MH.
(2) Analysis and interpretation of the data: IT, TM, and MH.
(3) Drafting of the article: IT, TM, and MH.
(4) Critical revision of the article for important intellectual content: IT and MH.
(5) Final approval of the article: IT, TM, and MH.
(6) Obtaining funding: TM and MH.
(7) Collection and assembly of data: IT and TM.

Funding

This work was supported by university and departmental funding sources.

Conflicts of interest

The authors report no conflicts of interest. The authors alone are responsible for the content and writing of the papers.

REFERENCES

1) Mobasheri A: Osteoarthritis year 2012 in review: biomarkers. Osteoarthritis Cartilage, 2012, 20: 1451–1464. [Medline] [CrossRef]
2) Teeple E, Jay GD, Elsaid KA, et al.: Animal models of osteoarthritis: challenges of model selection and analysis. AAPS J, 2013, 15: 438–446. [Medline] [CrossRef]
3) Hayami T, Pickarski M, Zhuo Y, et al.: Characterization of articular cartilage and subchondral bone changes in the rat anterior cruciate ligament transection and meniscectomized models of osteoarthritis. Bone, 2006, 38: 234–243. [Medline] [CrossRef]
4) Janusz MJ, Hookfin EB, Heitmeyer SA, et al.: Moderation of iodoacetate-induced experimental osteoarthritis in rats by matrix metalloproteinase inhibitors. Osteoarthritis Cartilage, 2001, 9: 751–760. [Medline] [CrossRef]
5) Lampropoulou-Adamidou K, Lelovas P, Karadimas EV, et al.: Useful animal models for the research of osteoarthritis. Eur J Orthop Surg Traumatol, 2014, 24: 263–271. [Medline] [CrossRef]
6) Jiang L, Li L, Geng C, et al.: Monosodium iodoacetate induces apoptosis via the mitochondrial pathway involving ROS production and caspase activation in rat chondrocytes in vitro. J Orthop Res, 2013, 31: 364–369. [Medline] [CrossRef]
7) Dunham J, Hoedt-Schmidt S, Kalbhen DA: Structural and metabolic changes in articular cartilage induced by iodoacetate. Int J Exp Pathol, 1992, 73: 455–464. [Medline]
8) Guzman RE, Evans MG, Bove S, et al.: Mono-iodoacetate-induced histologic changes in subchondral bone and articular cartilage of rat femorotibial joints: an animal model of osteoarthritis. Toxicol Pathol, 2003, 31: 619–624. [Medline] [CrossRef]
9) Bove SE, Calcaterra SL, Brooker RM, et al.: Weight bearing as a measure of disease progression and efficacy of anti-inflammatory compounds in a model of monosodium iodoacetate-induced osteoarthritis. Osteoarthritis Cartilage, 2003, 11: 821–830. [Medline] [CrossRef]
10) Scanzello CR, Goldring SR: The role of synovitis in osteoarthritis pathogenesis. Bone, 2012, 51: 249–257. [Medline] [CrossRef]
11) Matsuzaki T, Yoshida S, Kojima S, et al.: Influence of ROM exercise on the joint components during immobilization. J Phys Ther Sci, 2013, 25: 1547–1551. [Medline] [CrossRef]
12) Watanabe M, Hoso M, Hibino I, et al.: Histopathological changes of joint capsule after joint immobility compared with aging in rats. J Phys Ther Sci, 2010, 22: 369–374. [CrossRef]

13) Standring S: Gray's Anatomy, 40th ed. Amsterdam: Elsevier, 2008, pp 81–101.
14) Mainil-Varlet P, Aigner T, Brittberg M, et al. International Cartilage Repair Society: Histological assessment of cartilage repair: a report by the Histology Endpoint Committee of the International Cartilage Repair Society (ICRS). J Bone Joint Surg Am, 2003, 85A: 45–57. [Medline] [CrossRef]
15) Kim HK, Zbojniewicz AM, Merrow AC, et al.: MR findings of synovial disease in children and young adults: part 2. Pediatr Radiol, 2011, 41: 512–524. [Medline] [CrossRef]
16) Gerwin N, Bendele AM, Glasson S, et al.: The OARSI histopathology initiative—recommendations for histological assessments of osteoarthritis in the rat. Osteoarthritis Cartilage, 2010, 18: S24–S34. [Medline] [CrossRef]
17) Aigner T, Cook JL, Gerwin N, et al.: Histopathology atlas of animal model systems—overview of guiding principles. Osteoarthritis Cartilage, 2010, 18: S2–S6. [Medline] [CrossRef]
18) Pritzker KP, Gay S, Jimenez SA, et al.: Osteoarthritis cartilage histopathology: grading and staging. Osteoarthritis Cartilage, 2006, 14: 13–29. [Medline] [CrossRef]
19) Kurz B, Lemke AK, Fay J, et al.: Pathomechanisms of cartilage destruction by mechanical injury. Ann Anat, 2005, 187: 473–485. [Medline] [CrossRef]
20) Del Carlo M Jr, Loeser RF: Cell death in osteoarthritis. Curr Rheumatol Rep, 2008, 10: 37–42. [Medline] [CrossRef]
21) Qi JH, Ebrahem Q, Moore N, et al.: A novel function for tissue inhibitor of metalloproteinases-3 (TIMP3): inhibition of angiogenesis by blockage of VEGF binding to VEGF receptor-2. Nat Med, 2003, 9: 407–415. [Medline] [CrossRef]
22) Fransès RE, McWilliams DF, Mapp PI, et al.: Osteochondral angiogenesis and increased protease inhibitor expression in OA. Osteoarthritis Cartilage, 2010, 18: 563–571. [Medline] [CrossRef]
23) Zhang X, Crawford R, Xiao Y: Inhibition of vascular endothelial growth factor with shRNA in chondrocytes ameliorates osteoarthritis. J Mol Med Berl, 2016, 94: 787–798 in print. [Medline] [CrossRef]
24) Janusz MJ, Bendele AM, Brown KK, et al.: Induction of osteoarthritis in the rat by surgical tear of the meniscus: inhibition of joint damage by a matrix metalloproteinase inhibitor. Osteoarthritis Cartilage, 2002, 10: 785–791. [Medline] [CrossRef]
25) Kamekura S, Hoshi K, Shimoaka T, et al.: Osteoarthritis development in novel experimental mouse models induced by knee joint instability. Osteoarthritis Cartilage, 2005, 13: 632–641. [Medline] [CrossRef]
26) Ferland CE, Laverty S, Beaudry F, et al.: Gait analysis and pain response of two rodent models of osteoarthritis. Pharmacol Biochem Behav, 2011, 97: 603–610. [Medline] [CrossRef]
27) Pickarski M, Hayami T, Zhuo Y, et al.: Molecular changes in articular cartilage and subchondral bone in the rat anterior cruciate ligament transection and meniscectomized models of osteoarthritis. BMC Musculoskelet Disord, 2011, 12: 197. [Medline] [CrossRef]
28) Lories RJ: Joint homeostasis, restoration, and remodeling in osteoarthritis. Best Pract Res Clin Rheumatol, 2008, 22: 209–220. [Medline] [CrossRef]
29) van der Kraan PM, van den Berg WB: Osteophytes: relevance and biology. Osteoarthritis Cartilage, 2007, 15: 237–244. [Medline] [CrossRef]
30) Henrotin Y, Lambert C, Richette P: Importance of synovitis in osteoarthritis: evidence for the use of glycosaminoglycans against synovial inflammation. Semin Arthritis Rheum, 2014, 43: 579–587. [Medline] [CrossRef]
31) de Lange-Brokaar BJ, Ioan-Facsinay A, van Osch GJ, et al.: Synovial inflammation, immune cells and their cytokines in osteoarthritis: a review. Osteoarthritis Cartilage, 2012, 20: 1484–1499. [Medline] [CrossRef]
32) United Nations: Globally Harmonized System of Classification and Labelling of Chemicals (GHS) sixth revised edition. http://www.unece.org/fileadmin/DAM/trans/danger/publi/ghs/ghs_rev06/English/ST-SG-AC10-30-Rev6e.pdf (Accessed May 12, 2016)